TELKOMNIKA Indonesian Journal of Electrical Engineering
Vol.12, No.7, July 2014, pp. 4934 ~ 4943
DOI: 10.11591/telkomnika.v12i7.5629

Behavior of DFIG Wind Turbine during Unbalanced Grid Voltage

Omer Elfaki Elbashir*, Wang Zezhong, Liu Qihui
School of Electrical and Electronics Engineering
Telphone: +8613693044769, North China Electric Power University, Beijing, China
*Corresponding author, e-mail: omer.elbashir@yahoo.com

Abstract

The use of doubly fed induction generators (DFIGs) in wind turbines has become quite common for the last few years. These machines provide variable speed and are driven with a power converter which is sized for a small percentage of the turbine-rated power. This paper presents a detailed model of an induction generator coupled to wind turbine system. Modeling and simulation of the induction machine using vector control computing technique is done. DFIG wind turbine is an integrated part of the distributed generation system, therefore, any abnormality's associates with grid are going to affect the system performance considerably. Taking this into account, the performance of DFIG variable speed wind turbine under network fault is studied using simulation developed in MATLAB/SIMULINK.

***Keywords**: DFIG, d-q model, vector control*

1. Introduction

Wind power, one of the green, safe and low-carbon energy, is so fast developing in generating electricity that it has become the fourth major power source after coal, water and nuclear. It is also the only renewable power resource that owns over one hundred million kilowatt global installed capacity apart from water. The development of wind power brought about a series of problems at the same time, with the maintenance of wind turbines being the foremost [1].

DFIG is a new type of power generation system. The stator winding is connected with power frequency grid. The rotor winding is connected with three-phase alternating currents which frequency can be adjusted by controlling the current parameters of the rotor winding, not only keep the same frequency, but also the grid power factor can be adjusted to improve the stability of the system [2].

For the dynamic feature, the DFIG becomes the most popular generator for wind power generation system. Firstly, DFIG can supply power to the grid at constant voltage and constant frequency while the rotor can operate at sub-synchronous mode or super-synchronous mode. Secondly, the rating of the power converter is only about 30% of the rated power of the wind turbine. At third, the generated active and reactive power can be controlled independently. For conventional wind farms connected to an electric network, the turbines are disconnected from the grid if voltage unbalance of 6% or more is detected [3]. Then, the continuity of the power generation in the wind energy system may be affected by tripping the wind turbine from the utility grid. Hence it is desirable to implement the generator control system to withstand to a certain level of voltage unbalances. If the voltage unbalance is not taken into account in the control system, a highly unbalanced stator current could be produced even with a small unbalanced stator voltage [4].

DFIGs are commonly used for large wind turbines operating at variable speed. For maintaining continuous operation of such wind turbines during power system disturbances, i.e., fault ride through capability, extensive studies have been carried out in the last few years. However, symmetrical voltages are considered in most cases. In reality, asymmetric faults occur more frequently than symmetric faults in transmission system. The stator current of a DFIG could be highly unbalanced even with a small unbalanced grid voltage if no unbalance control were considered. The unbalanced voltage and current cause a number of problems such as

Received September 3, 2013; Revised February 3, 2014; Accepted March 16, 2014

overheating of stator windings, extra mechanical stresses due to torque pulsation, and output power pulsations [5-6].

Many new wind farms will employ wind turbines based on DFIG, which offer several advantages when compared with fixed-speed generators [7-10]. These advantages, including speed control, reduced flicker, and four-quadrant active and reactive power capabilities, are primarily achieved via control of a rotor side converter (RSC), which is typically rated at around 30%–35% of the generator rating for a given rotor speed variation range of $\pm 25\%$. The steady-state response and performance of DFIG-based wind turbines are now well understood [7, 11, 13]. DFIG systems are conventionally controlled using either stator voltage-oriented [7, 8] or stator flux-oriented [9, 12] controls based on d-q decoupling. For most of the studies reported, symmetric stator voltage supply was assumed even during network disturbance. For small wind farms connected to a distribution network, it is required that they can withstand a steady-state maximum value of phase voltage unbalance of 2% without tripping [14].

2. Dynamic d-q Model of Induction Generator

The $d-q$ axis representation of an induction generator is used for simulation, taking flux linkage as a basic variable. It is based on fifth-order two axis representations commonly known as the "Park model" [15]. Here an equivalent 2-phase machine represents 3-phase machine, where $d^s - q^s$ correspond to the stator direct and quadrature axes, and $d^r - q^r$ correspond to the rotor direct and quadrature axes and a synchronously rotating $d-q$ reference frame is used with the direct $d-axis$ oriented along the stator flux position.

A symmetrical 3-phase induction machine with stationary axes as, bs, cs separated by an angle $2\pi/3$ is considered. Assume that the $d^s - q^s$ axes are oriented at angle θ. If the synchronously rotating $d-q$ axes rotate at a synchronous speed ω_e with respect to $d^s - q^s$ axes, then the voltages on the $d^s - q^s$ axes can be converted into $d-q$ a synchronously rotating frame as follows:

$$\begin{aligned} v_{qs} &= v_{qs}^s \cos\theta_e - v_{ds}^s \sin\theta_e \\ v_{ds} &= v_{qs}^s \sin\theta_e + v_{ds}^s \cos\theta_e \end{aligned} \qquad (1)$$

Resolving the rotating frame parameters into stationary frame:

$$\begin{aligned} v_{qs}^s &= v_{qs} \cos\theta_e + v_{ds} \sin\theta_e \\ v_{ds}^s &= -v_{qs} \sin\theta_e + v_{ds} \cos\theta_e \end{aligned} \qquad (2)$$

According to Kron's equation, the stator circuit equations are:

$$\begin{aligned} v_{qs}^s &= R_s i_{qs}^s + \frac{d}{dt}\lambda_{qs}^s \\ v_{ds}^s &= R_s i_{ds}^s + \frac{d}{dt}\lambda_{ds}^s \end{aligned} \qquad (3)$$

Where λ_{qs}^s is the $q-axis$ stator flux linkage, and λ_{ds}^s is the $d-axis$ stator flux linkage respectively. Convert equation (3) to the synchronous rotating frame, we get:

$$v_{qs} = R_s i_{qs} + \frac{d}{dt}\lambda_{qs} + (\omega_e \lambda_{ds})$$
$$v_{ds} = R_s i_{ds} + \frac{d}{dt}\lambda_{ds} - (\omega_e \lambda_{qs}) \tag{4}$$

The machine rotor equations can be written in a similar way as the stator equations:

$$v_{qr} = R_r i_{qr} + \frac{d}{dt}\lambda_{qr} + (\omega_e \lambda_{dr})$$
$$v_{dr} = R_r i_{dr} + \frac{d}{dt}\lambda_{dr} - (\omega_e \lambda_{qr}) \tag{5}$$

If we put $(\omega_e - \omega_r)$ in the place of ω_e Equation (5) becomes:

$$v_{qr} = R_r i_{qr} + \frac{d}{dt}\lambda_{qr} + (\omega_e - \omega_r)\lambda_{dr}$$
$$v_{dr} = R_r i_{dr} + \frac{d}{dt}\lambda_{dr} - (\omega_e - \omega_r)\lambda_{qr} \tag{6}$$

$$\lambda_{qs} = L_{ls} i_{qs} + L_m (i_{qs} + i_{qr}) = L_s i_{qs} + L_m i_{qr} \tag{7}$$

$$\lambda_{ds} = L_{ls} i_{ds} + L_m (i_{ds} + i_{dr}) = L_s i_{ds} + L_m i_{dr} \tag{8}$$

$$\lambda_{qr} = L_{lr} i_{qr} + L_m (i_{qs} + i_{qr}) = L_r i_{qr} + L_m i_{qs} \tag{9}$$

$$\lambda_{dr} = L_{lr} i_{dr} + L_m (i_{ds} + i_{dr}) = L_r i_{dr} + L_m i_{ds} \tag{10}$$

3. RSC Control

The main purpose of the RSC is to maintain the rotor speed constant irrespective of the wind speed and also the control strategy has been implemented to control the active and reactive powers flow of the machine using the rotor current components. The active power flow is controlled through i_{dr} and the reactive power flow is controlled through i_{qr}. The standard voltage oriented vector control strategy is used for the RSC to implement control action. Here the real axis of the stator voltage is chosen as the d-axis. Since the stator is connected to the utility grid and the influence of stator resistance is small, the stator magnetizing current i_m can be considered as constant. Under voltage orientation, the relationship between the torque and the $d-q$ axis voltages, currents and fluxes can be written with neglecting of leakage inductances $(L_{ls} = 0)$. To maximize the turbine output power, DFIG must be controlled through the control of i_{dr} and i_{qr}. To simplify the control and calculate i_{dr}^*, the stator flux component λ_{ds} is set to zero.

$$\begin{aligned}
\lambda_{ds} &= 0 \\
\lambda_{qs} &= L_s i_{qs} + L_m i_{qr} \\
&= (L_{ls} + L_m) i_{qs} + L_m i_{qr} \\
&= L_{ls} i_{qs} + (i_{qs} + i_{qr}) L_m \\
&= L_m i_m
\end{aligned} \tag{11}$$

The equations of rotor fluxes are:

$$\lambda_{qr} = \frac{L_m}{L_s}\lambda_{qs} + \sigma L_r i_{qr} = \frac{L_m^2}{L_s} i_m + \sigma L_r i_{qr}$$
$$\lambda_{dr} = \frac{L_m}{L_s}\lambda_{ds} + \sigma L_r i_{dr} = \sigma L_r i_{dr} \tag{12}$$

Where $\sigma = 1 - \frac{L_m^2}{L_s L_r}$

By substituting the values of λ_{dr} and λ_{qr} from equation (12) in equation (6), the rotor voltages are:

$$v_{qr} = R_r i_{qr} + \sigma L_r \frac{d}{dt} i_{qr} + (\omega_e - \omega_r)\sigma L_r i_{dr} \tag{13}$$

$$\begin{aligned} v_{dr} &= R_r i_{dr} + \sigma L_r \frac{d}{dt} i_{dr} - (\omega_e - \omega_r)\left(\frac{L_m^2}{L_s} i_m + \sigma L_r i_{qr}\right) \\ &= R_r i_{dr} + \sigma L_r \frac{d}{dt} i_{dr} - (\omega_e - \omega_r)\left(L_{equ.} i_m + \sigma L_r i_{qr}\right) \end{aligned} \tag{14}$$

Where $L_{equ.}$ is the equivalent inductance.

v'_{dr} and v'_{qr} can be found from the current errors processing through standard PI controllers and the reference current i^*_{dr} can be found either from the reference torque or from the speed errors through standard PI controllers. Similarly i^*_{qr} can be found from the reactive power errors. The active power and the speed are controlled using the current control loop. The electromagnetic torque can be expressed as:

$$T_e = \frac{3}{2} P \frac{L_m}{L_s} \lambda_{qs} i_{dr} \tag{15}$$

The value of i^*_{dr} can be found using Equation (15):

$$i^*_{dr} = \frac{T_e^* L_s}{\lambda_{qs} L_m} \tag{16}$$

Figure 1 below shows the RSC with the vector control.

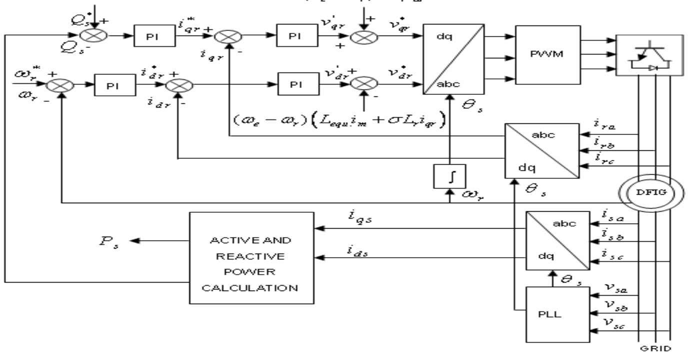

Figure 1. Vector Control Struture of RSC

4. Modeling and Simulation

4.1. Modeling of DFIG System

The voltage equations of an induction machine in arbitrary reference frame can be written in terms of the currents as:

$$\begin{bmatrix} v_{qs} \\ v_{ds} \\ v_{0s} \\ v'_{qr} \\ v'_{dr} \\ v'_{0r} \end{bmatrix} = \begin{bmatrix} R_s+\frac{P}{\omega_b}X_{ss} & \frac{\omega}{\omega_b}X_{ss} & 0 & \frac{P}{\omega_b}X_m & \frac{\omega}{\omega_b}X_m & 0 \\ -\frac{\omega}{\omega_b}X_{ss} & R_s+\frac{P}{\omega_b}X_{ss} & 0 & -\frac{\omega}{\omega_b}X_m & \frac{P}{\omega_b}X_m & 0 \\ 0 & 0 & R_s+\frac{P}{\omega_b}X_{ls} & 0 & 0 & 0 \\ -\frac{P}{\omega_b}X_m & \frac{\omega-\omega_r}{\omega_b}X_m & 0 & R_r+\frac{P}{\omega_b}X_{rr} & \frac{\omega-\omega_r}{\omega_b}X_{rr} & 0 \\ -\frac{\omega-\omega_r}{\omega_b}X_m & \frac{P}{\omega_b}X_m & 0 & -\frac{\omega-\omega_r}{\omega_b}X_{rr} & R_r+\frac{P}{\omega_b}X_{rr} & 0 \\ 0 & 0 & 0 & 0 & 0 & R_r+\frac{P}{\omega_b}X_{lr} \end{bmatrix} \begin{bmatrix} i_{qs} \\ i_{ds} \\ i_{0s} \\ i'_{qr} \\ i'_{dr} \\ i'_{0r} \end{bmatrix} \quad (17)$$

Where v_{qs}, v_{ds} are q-axis and d-axis stator voltages, i_{qs}, i_{ds} are q-axis and d-axis stator currents, v'_{qr}, v'_{dr}, i'_{qr} and i'_{dr} are q-axis and d-axis rotor voltages and currents referred to the stator windings by appropriate turns ratio, ω is the rotating speed of the arbitrary reference frame, ω_r is the rotor speed, X_{ss}, X_{rr} are stator and rotor self inductive reactances, X_m is the mutual reactance, and X_{ls}, X_{lr}, R_s and R_r are stator and rotor leakage reactances and resistances.

The swing equation is:

$$T_e = 2H\omega_r + T_m \quad (18)$$

Where T_m is the mechanical torque and H is the inertia.

The doubly fed induction generator model consists of Equation (17), the swing Equation (18), and rotor side controller. The complete DFIG system with controllers is modeled in Matlab/Simulink. The inputs of the model are voltage and rotor speed, mechanical torque and the output is a current vector and electromagnetic torque. The simulink model of DFIG system is shown in Figure 2 below.

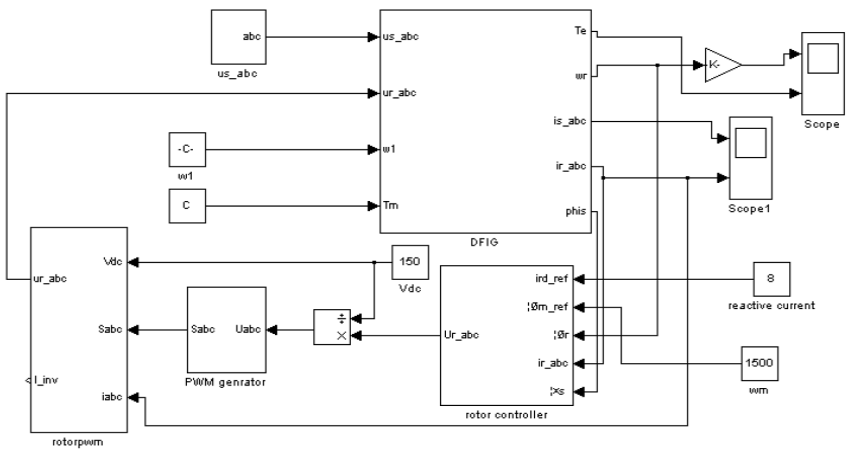

Figure 2. Simulink Model of DFIG System

5. Results and Discussion

The induction machine is simulated using MATLAB/SIMULINK environment. The performance of the DFIG system is analyzed under disturbance of the grid voltage. The main objective of this Work is to study the performance analysis of the DFIG for a wind turbine application during voltage fluctuations. The voltage fluctuations are made by lowering and raising the voltage values in the utility grid intentionally for simulation keeping in view of different grid disturbances.

5.1. Simulation Under Normal Condition

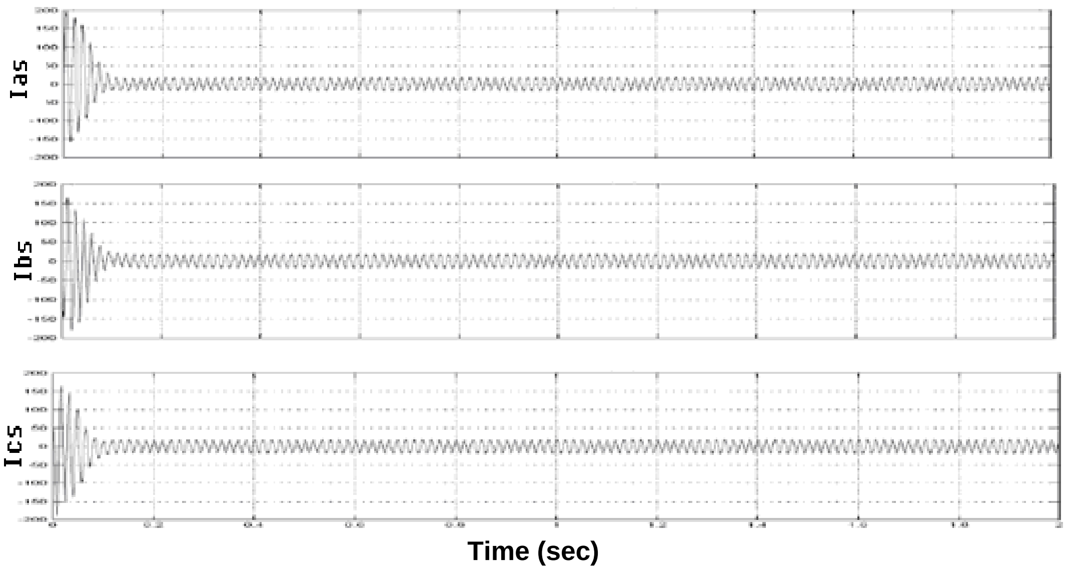

Figure 3. Stator Currents during Balance Condition

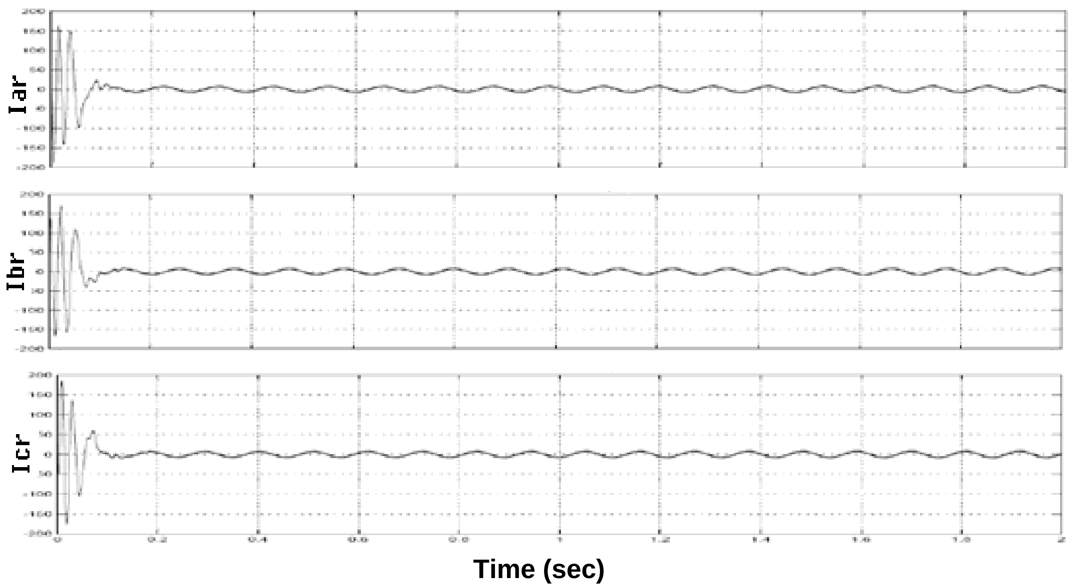

Figure 4. Rotor Currents during Balance Condition

5.1.1. Discussion

The transient torque and speed characteristics with time are different from the steady state torque and speed characteristics with time shown in Figure 5. The variation in instantaneous torque is due to the transient offset in stator currents. Although the offset in each of the currents depends upon the value of source voltage at the time of application. The instantaneous torque is independent of the initial values of balanced source voltage because the machine is symmetrical. Also machine currents varies during transient period. due to the interaction of the stator and rotor electric transients.

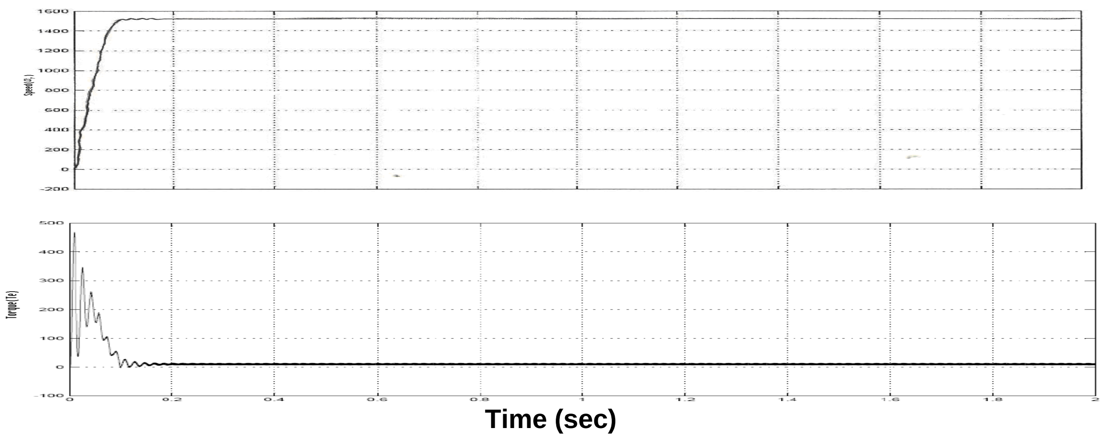

Figure 5. Speed and Torque during Balance Condition

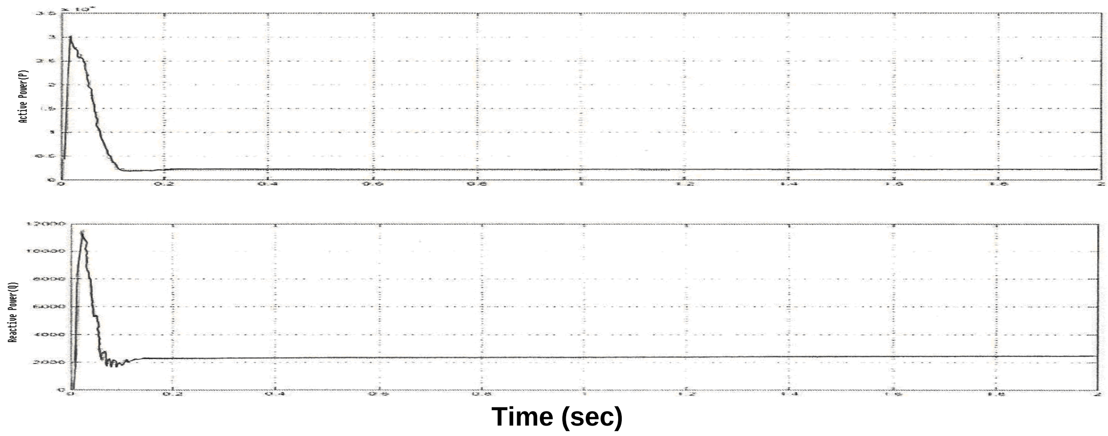

Figure 6. Active and Reactive Power during Balance Condition

5.2. Simulation under Voltage Dip

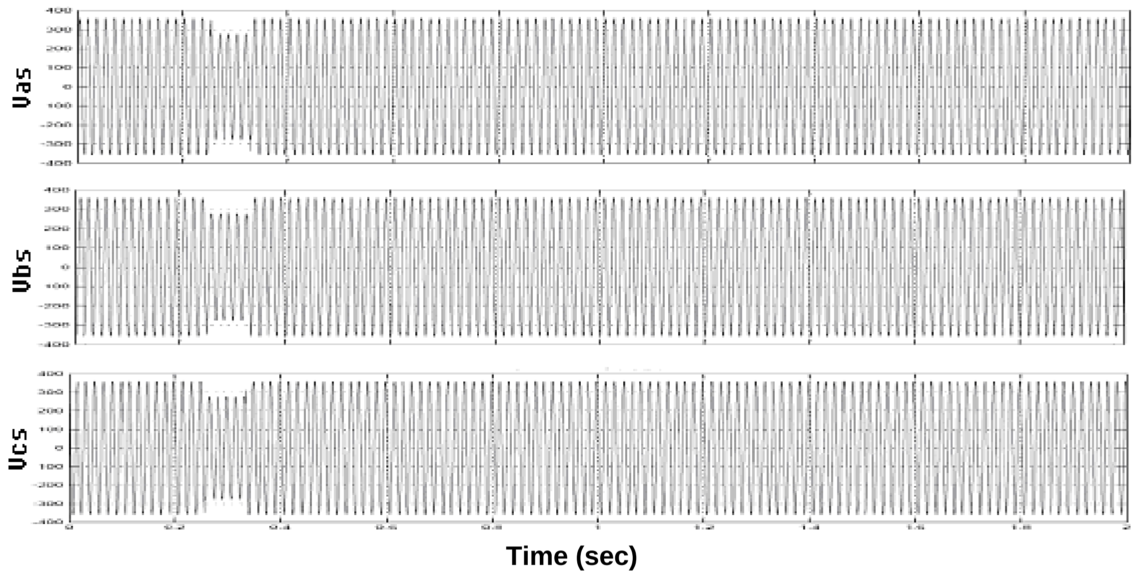

Figure 7. Stator Voltage during Voltage Dip

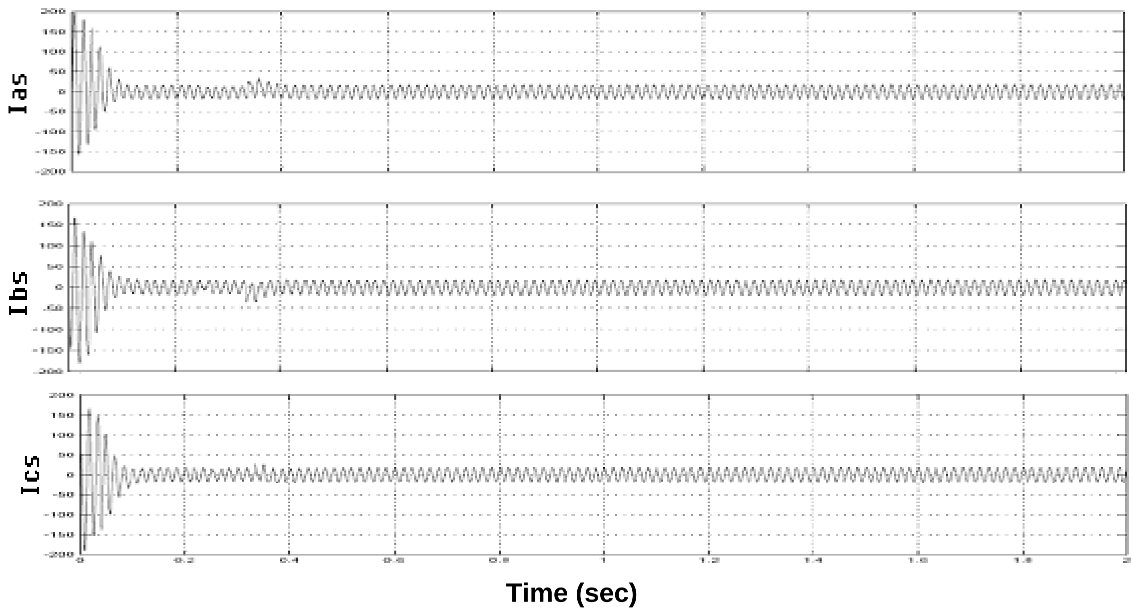

Figure 8. Stator Currents during Voltage Dip

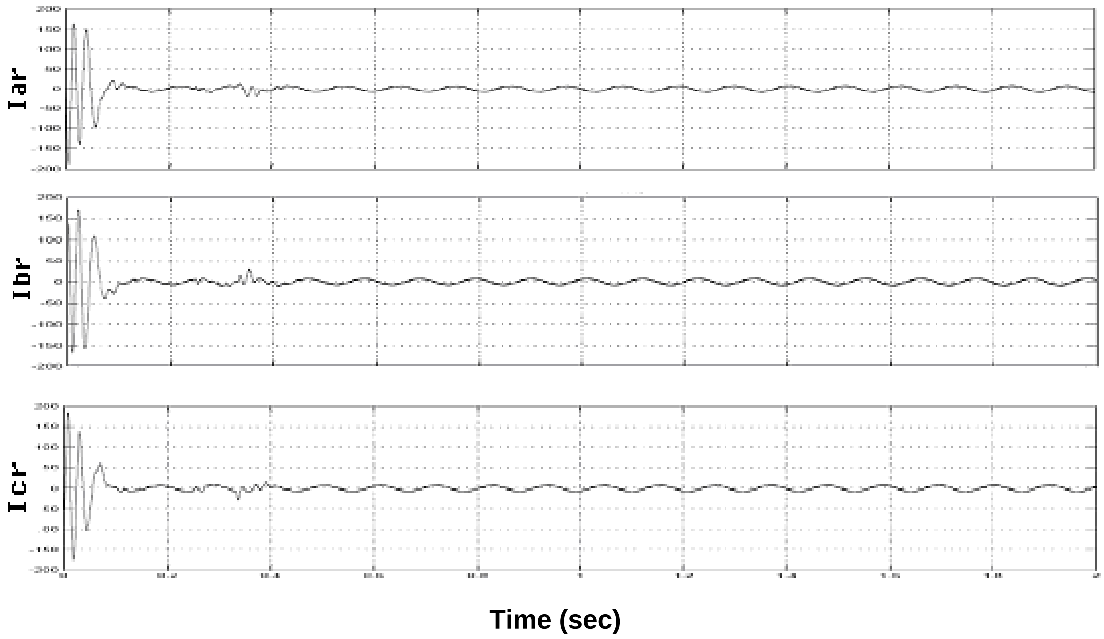

Figure 9. Rotor Currents during Voltage Dip

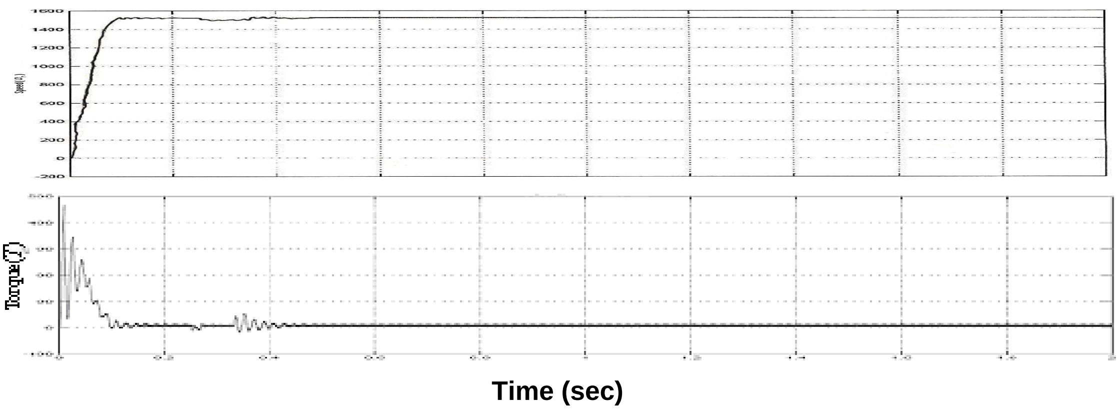

Figure 10. Speed and Torque during Voltage Dip

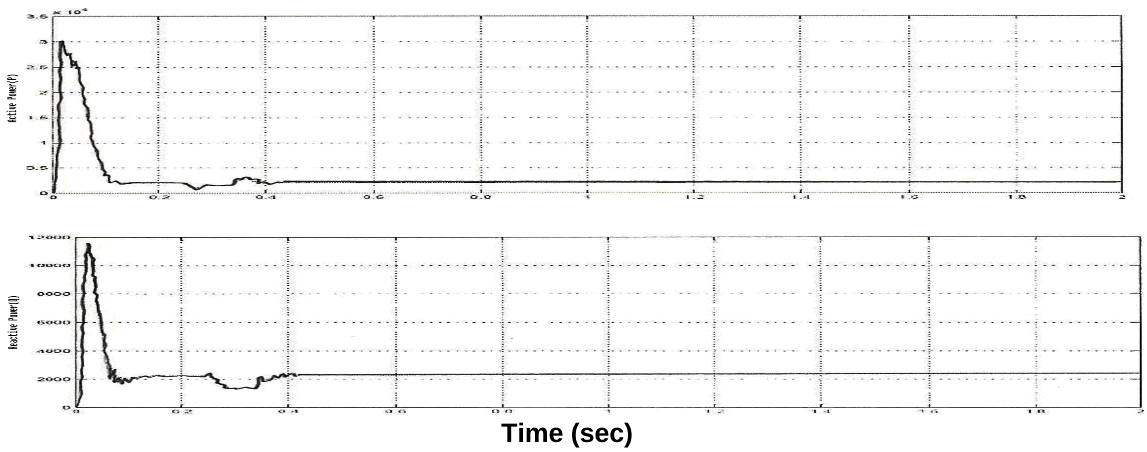

Figure 11. Active and Reactive Power during Voltage Dip

5.2.1. Discussion

In Figure 9, the rotor currents of the machine are shown for a voltage dip of 85%, implying, that only 15% of the grid voltage remains. It can be seen that the rotor currents oscillates to about four times the rated current. This implies that a voltage dip can cause high induced voltages or currents in the rotor circuit. These currents might destroy the converter, if nothing is done to protect it.

6. Conclusion

The dynamic behavior of DFIG under power system disturbance was simulated using MATLAB/SIMULINK. The DFIG considered in this analysis is a wound rotor induction generator with slip rings. The stator is directly connected to the grid and the rotor is interface via a back to back power converter. Power converter are usually controlled utilizing vector control techniques which allow the decoupled control of both active and reactive power flow to the grid. In the present investigation, the dynamic DFIG performance is presented for both normal and abnormal grid conditions. The control performance of DFIG is satisfactory in normal grid conditions and it is found that, both active and reactive power maintains a study pattern in spite of fluctuating wind speed and the net of the electrical power supplied to grid is maintained constant.

References

[1] Zhai Yongjie, Wang Dong feng, Zhang Junying, Han Yuejiao. Research on early fault diagnostic method of wind turbines. *TELKOMNIKA Indonesian Journal of Electrical Engineering.* 2013; 11(5): 330 -2341.

[2] Ding Shuye, Zhang Ning. Analysis of electromagnetic properties of doubly-fed turbine generator. *TELKOMNIKA* Indonesian Journal of Electrical Engineering. 2013; *Vol. 11, Issues 2, page 783 -788.*

[3] T Brekken, N Mohan. *A novel doubly-fed induction wind generator control scheme for reactive power control and torque pulsation compensation under unbalanced grid voltage conditions. IEEE PESC Conf Proc.,* 2003*; 2: 760-764*.

[4] L Xu, Y Wang. Dynamic modeling and control of DFIG-based wind turbines under unbalanced network conditions. *IEEE Trans. on Power System,* 2007*;* 22, 1: 314*–323.*

[5] FM Hughes, O Anaya-Lara, N Jenkins, G Strbac. Control of DFIG based wind generation for power network support. *IEEE Trans. On Power Systems,* 2005*; 20; 1958-1966.*

[6] S Seman, J Niiranen, S Kanerva, A Arkkio, J Saitz. Performance study of a doubly fed wind-power induction generator Under Network Disturbances. *IEEE Trans. on Energy Conversion.* 2006*;* 21: 883-890.

[7] T Thiringer, A Petersson, T Petru. *Grid disturbance response of wind turbines equipped with induction generator and doubly-fed induction generator.* Proc. *IEEE Power Engineering Society General Meeting,* 2003*; 3: 13-17.*

[8] T Sun, Z Chen, F Blaabjerg. Voltage recovery of grid-connected wind turbines with DFIG after a short-circuit fault. *Proc. 35th IEEE POWER Electronics Specialists Conference* 2004*; 3: 1991-1997.*

[9] S Muller, M Deicke, RW De Doncker. Doubly fed induction generator systems for wind turbines. *IEEE Ind. Appl. Mag.,* 2002*; 8(3): 26–33.*

[10] H Akagi H Sato. Control and performance of a doubly-fed induction machine intended for a fly wheel energy storage system. *IEEE Trans. Power Electron.,* 2002*;* 17(1): 109–116*.*

[11] R Pena, JC Clare, GM Asher. Double fed induction generator using back-to-back PWM converter and its application to variable- speed wind-energy generation. Proc. Inst. Elect. Eng., 1996; 143(3): 231-241.

[12] M Yamamoto, O Motoyoshi. Active and reactive power control for doubly-fed wound rotor induction generator. *IEEE Trans. Power Electron.,* 1991; 6(4): 624–629*.*

[13] JB Ekanayake, L Holdsworth, XG Wu, N Jenkins. Dynamic modeling of doubly fed induction generator wind turbines. *IEEE Trans. Power Syst.,* 2003; 18(2): 803–809.

[14] National Grid Transco, Appendix 1, Extracts from the Grid Code-Connection Conditions. 2004. Available: http://www. nationalgrid.com.

[15] GR Slemon. Modelling induction machines for electric drives. *IEEE Transaction on Industry Application.* 1989; 25(6): 1126-1131.